

Geothermics

Prof. Magdala Tesauro

Course Outline:

1. Thermal conditions of the early Earth and present-day Earth's structure
2. Thermal parameters of the rocks
3. Thermal structure of the lithospheric continental areas (steady state)
4. Thermal structure of the lithospheric oceanic areas
5. Thermal structure of the lithosphere for transient conditions in various tectonic settings
- 6. Heat balance of the Earth**
7. Thermal structure of the sedimentary basins
8. Thermal maturity of sediments
9. Mantle convection and hot spots
10. Magmatic processes and volcanoes
11. Heat transfer in hydrogeological settings
12. Geothermal Systems



UNIVERSITÀ
DEGLI STUDI
DI TRIESTE

Global Energy Budget

$$\frac{d(U + E_c + E_g)}{dt} = - \int_S \mathbf{q} \cdot \mathbf{n} dS + \int_V H dV - p_a \frac{dV}{dt} + \int_V \Phi dV.$$

Different energy components

All processes contributing to energy changes

U=internal energy, E_c =kinetic energy, E_g =gravitational potential energy

n=unit normal vector, S=outer surface of the Earth, V=total volume of the Earth

q=surface heat flux, H=internal heat generation, p_a =the work of atmospheric pressure (due to planet's contraction), ϕ =energy transfers to or from external systems (e.g., tidal dissipation).

E_g =energy required to bring matter to infinity

For the Earth, assuming a spherical symmetry:
$$E_g = - \int_0^R \rho(r)g(r)r4\pi r^2 dr.$$

For a sphere with uniform density and same mass of the Earth:
$$E_g = -\frac{3}{5} \frac{GM^2}{R}.$$

- For the Earth E_g is negative because the accretion process releases energy
- E_g changes, due to thermal contraction, chemical differentiations, and vertical variations of the Earth's surface are compensated by strain energy (E_s , the energy required to compress matter to its present local pressure) changes.

Energy components

Kinetic energy

$$E_c = E_{\text{rot}} + E_{\text{contr}} + E_{\text{conv}}$$

(E_{contr} and E_{conv} are negligible)

E_{rot} =energy due to Earth's rotation (main component), E_{contr} =energy due to radial contraction, E_{conv} =energy due to internal convective motions

Energy components

	Value	Units
Rotational energy	$2.1 \times 10^{29} \dagger$	J
Internal energy (for 2500 K average temperature)	1.7×10^{31}	J
Gravitational energy (uniform sphere)	$2.2 \times 10^{32} \dagger$	J
Rotation angular velocity	7.292×10^{-5}	rad s ⁻¹
Polar moment of inertia	8.036×10^{37}	kg m ²
Total mass	5.974×10^{24}	kg
Total volume	1.08×10^{21}	m ³
Mass mantle	$\approx 4.0 \times 10^{24}$	kg
Mass crust	$\approx 2.8 \times 10^{22}$	kg
Mass core	$\approx 1.95 \times 10^{24}$	kg

Sources of heat loss: tidal heating and crust-mantle differentiation

Tidal heating

- Earth's rotation is accelerating because of postglacial readjustments, and it is slowing down because of tidal interaction with the moon.
- Tidal interaction with the moon causes loss of the rotational and gravitational potential energy, which is converted into heat by frictional forces.
- The slowing down of Earth's rotation is $5.4 \times 10^{-22} \text{ rad s}^{-1}$, leading to 0.024 ms yr^{-1} increase in the length of the day. The energy loss has been calculated to be 3 TW, which must be accounted by dissipation in the oceans (mostly in the shallow seas), in the solid earth, and in the Moon.

Crust-mantle differentiation

Some gravitational potential energy is also released by the extraction of continental crust out of the mantle:

This energy loss is obtained by considering the potential energy of a differentiated Earth:

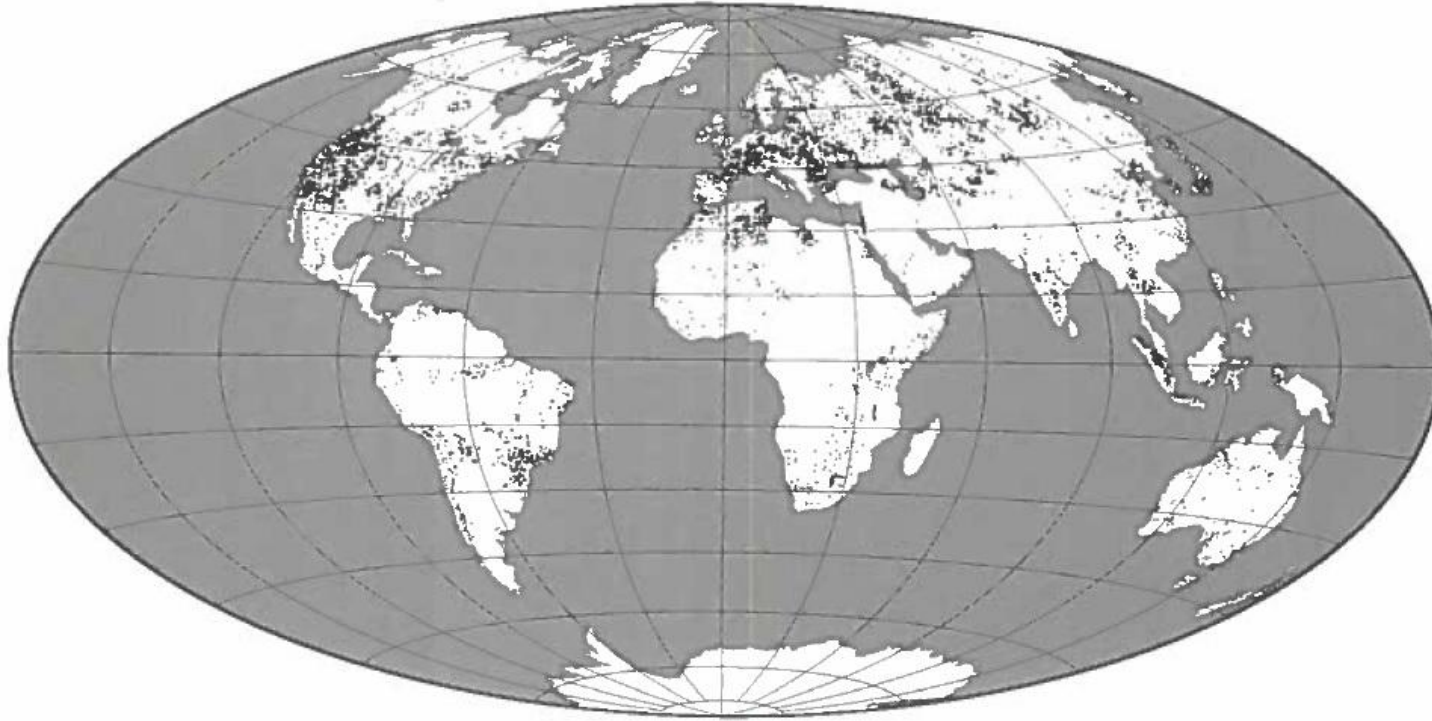
$$E_{\text{gm}} = - (3/5) GM_{\text{m}}^2 / R_1 - GM_{\text{m}} M_{\text{c}} / R_1$$

M_{c} is the mass of crust ($\sim 2.6 \times 10^{22} \text{ kg}$) and residual material with mass M_{m} is in a sphere of radius R_1 .

- For a constant rate of crustal growth during 3 Gyr, the contribution to the energy budget is small, 0.1TW. If the crust differentiated in two or three short episodes, each episode may have added as much as 1TW to the mantle budget.

Heat loss through continents

- Continental heat flux data are uneven distributed (most of data are in the north hemisphere) and the mean is 80 mWm^{-2} .
- Weighing the heat flux data by area sampling, bias are removed and the mean becomes $\sim 65 \text{ mWm}^{-2}$
- The contribution of all the continental areas ($210 \times 10^6 \text{ km}^2$) to the energy loss of the Earth is $\sim 14 \text{ TW}$.



Continental heat flux statistics †

	$\mu(Q)$ mW m^{-2}	$\sigma(Q)$ mW m^{-2}	$N(Q)$
World			
all values	79.7	162	14123
averages $1^\circ \times 1^\circ$	65.3	82.4	3024
averages $2^\circ \times 2^\circ$	64.0	57.5	1562
averages $3^\circ \times 3^\circ$	63.3	35.2	979
USA			
all values	112.4	288	4243
averages $1^\circ \times 1^\circ$	84	183	532
averages $2^\circ \times 2^\circ$	78.3	131.0	221
averages $3^\circ \times 3^\circ$	73.5	51.7	128
without USA			
all values	65.7	40.4	9880
averages $1^\circ \times 1^\circ$	61.1	30.6	2516
averages $2^\circ \times 2^\circ$	61.6	31.6	1359
averages $3^\circ \times 3^\circ$	61.3	31.3	889

† μ is the mean, σ is the standard deviation and N is the number of values

Heat loss through continents

- Present surface heat flux data from submerged and recently active continental areas ($92 \times 10^6 \text{ km}^2 \sim 45\%$ of the continental surface) reflect the heat from the mantle in the past 200 Myr.
- In zone of extension lithospheric thinning enhance heat flux, reflecting the contribution of the transient component and mantle usually shows short wavelength variations, due to cooling of shallow magmatic bodies and/or groundwater movements.
- In compressional orogens, lithospheric thickening result in reduced temperature gradients and heat flux, but total heat production is larger.
- The average heat flux of the continental margins (78 mW m^{-2}), higher than in stable regions despite the thinner crust, is explained by the cooling of the stretched lithosphere and is reflected in thermal subsidence.

*Estimates of bulk continental crust heat production from heat flux data
(Jaupart and Mareschal, 2003)*

Age group	Heat production $\mu\text{W m}^{-3}$	Total (40 km crust) mW m^{-2}	% Area †
Archean	0.56–0.73	23–30	9
Proterozoic	0.73–0.90	30–37	56
Phanerozoic	0.95–1.21	37–47	35
Total Continents	0.79–0.99	32–40	100

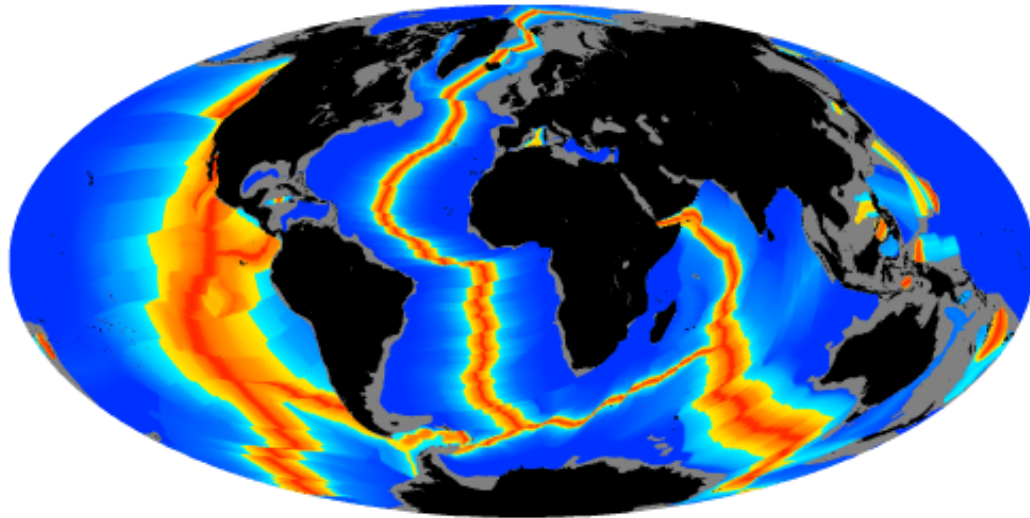
† Fraction of total continental surface, from Model 2 in Rudnick and Fountain (1995).

Surface area and heat flux in oceans and continents

	Area	Total heat flux
Oceans		
Oceanic	$273 \times 10^6 \text{ km}^2$	
Marginal basins	$27 \times 10^6 \text{ km}^2$	
Total oceans	$300 \times 10^6 \text{ km}^2$	32 TW
Continents		
Precambrian	$95 \times 10^6 \text{ km}^2$	
Paleozoic	$23 \times 10^6 \text{ km}^2$	
Stable continental	$118 \times 10^6 \text{ km}^2$	
Active continental	$30 \times 10^6 \text{ km}^2$	
Submerged (margins and basins)	$62 \times 10^6 \text{ km}^2$	
Total continental	$210 \times 10^6 \text{ km}^2$	14 TW

Oceanic heat flux

To reduce/cancel errors measurements heat flux values are binned in age intervals of 2Myr



Surface heat flux (Q) decreases with age (τ):

$$Q(\tau) = C_Q \tau^{-1/2}$$

$$Q(\tau) = \lambda T_M / \sqrt{\pi \kappa \tau}$$

For constant properties

For age > 80Myr heat flux is almost constant: $q_{80} \sim 48 \text{ mWm}^{-2}$

C_Q = constant valid for arbitrary temperature-dependent physical properties

T_M = Potential T of oceanic upper mantle

Potential temperature of the oceanic upper mantle

T , °C	Reference	Method
1315	McKenzie <i>et al.</i> (2005)	Depth + heat flux with cooling model
1280	McKenzie and Bickle (1988)	Average basalt composition
1315–1475	Kinzler and Grove (1992)	Basalt composition

Heat flow measurements on the sea floor are done (1) by dropping a probe (consisting of 15 m long shaft fitted with thermistors), penetrating the soft sediments of sea floor and measuring T ; (2) deep-sea drill-holes (only in a small number of sites).

Oceanic heat loss

$$Q_0 = \int_0^{\tau_{\max}} q(\tau) \frac{dA}{d\tau} d\tau \quad \frac{dA_1}{d\tau} = C_A(1 - \tau/\tau_m)$$

$A(\tau)$ =distribution of sea floor with age (obtained from maps of magnetic anomalies)

$\tau_m = 180$ Myr

C_A (plate accretion rate ~ 3.34 - 3.45 $\text{km}^2\text{yr}^{-1}$) can be different if marginal basins are included or not in the calculations. Marginal basins represent 3% of the oceanic surface and cause an uncertainty on the heat loss estimate of $\sim 1\%$.

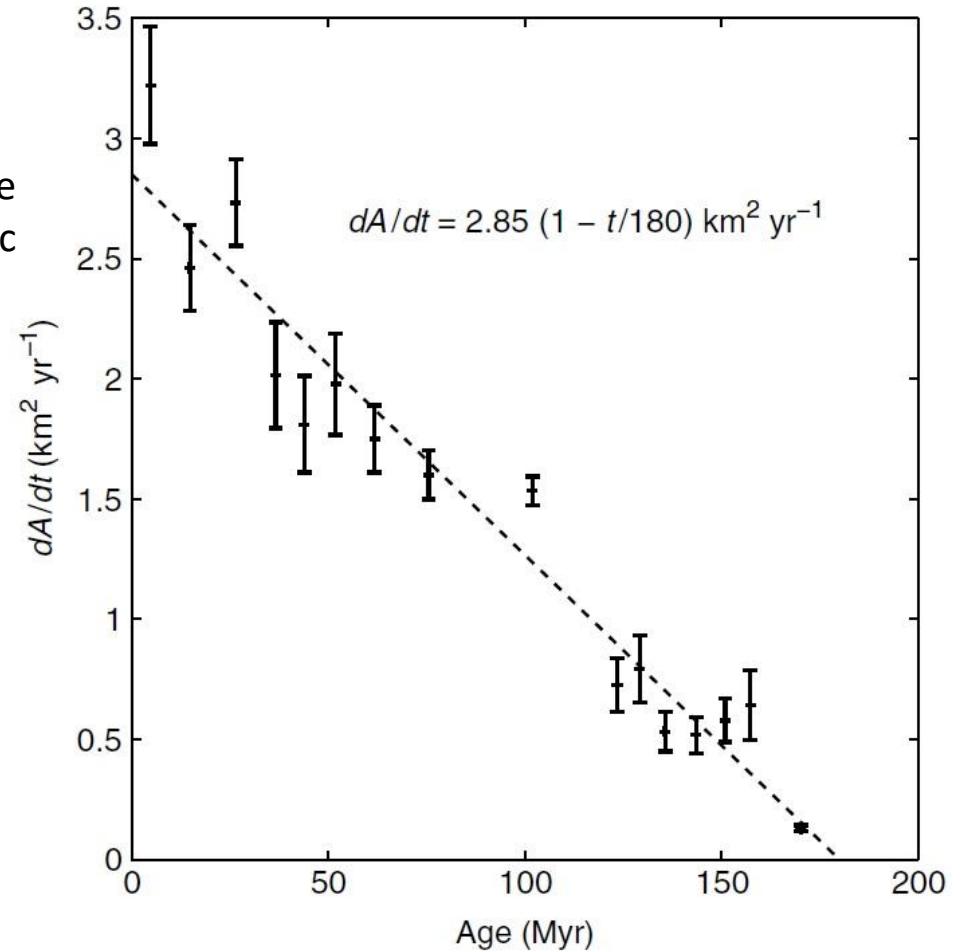
Estimates of the continental and oceanic heat flux and global heat loss

	Continental mW m^{-2}	Oceanic mW m^{-2}	Total TW
Williams and von Herzen (1974)	61	93	43
Davies (1980)	55	95	41
Sclater <i>et al.</i> (1980a)	57	99	42
*Pollack <i>et al.</i> (1993)	65	101	44
Jaupart <i>et al.</i> (2007)†	65	94	46

† The average oceanic heat flux does not include the contribution of hot spots. The total heat loss estimate does include 3 TW from oceanic hot spots.

*These estimate were based on $T_M = 1725$ K and $C_Q = 510$ $\text{mWm}^{-2}\text{My}^{1/2}$

Distribution of sea floor area with age



Oceanic area (exluding marginal basins): $257 \times 10^6 \text{ km}^2$

Oceanic heat loss

$$Q_0 = \int_0^{\tau_{\max}} q(\tau) \frac{dA}{d\tau} d\tau \quad \frac{dA_1}{d\tau} = C_A(1 - \tau/\tau_m)$$

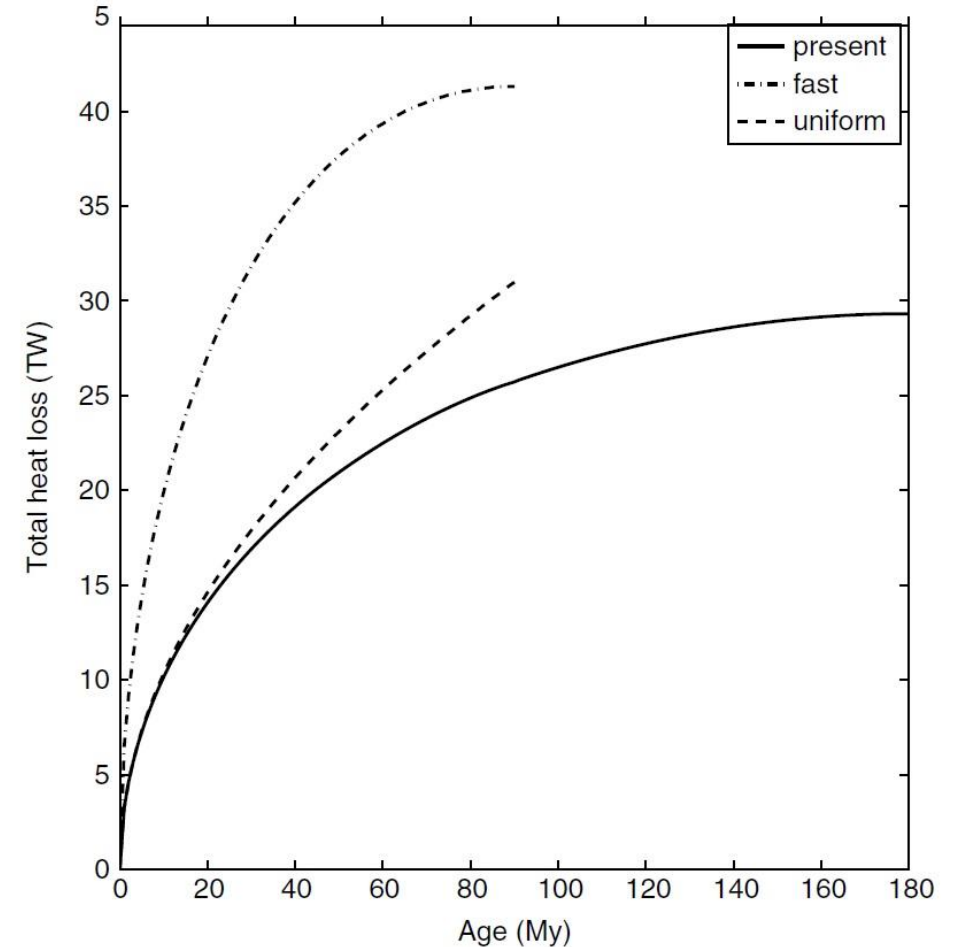
$$Q(\tau) = C_Q \tau^{-1/2}$$

Integrating sea floor younger and older than 80 Myr:

$$Q_{80-} = \int_0^{80} C_Q \tau^{-1/2} C_A(1 - \tau/180) d\tau = 24.3 \text{ TW}$$

$$Q_{80+} = q_{80} \int_{80}^{180} C_A(1 - \tau/180) dt' = 4.4 \text{ TW}$$

$$Q_{\text{oceans}} = 29 \pm 1 \text{ TW}$$

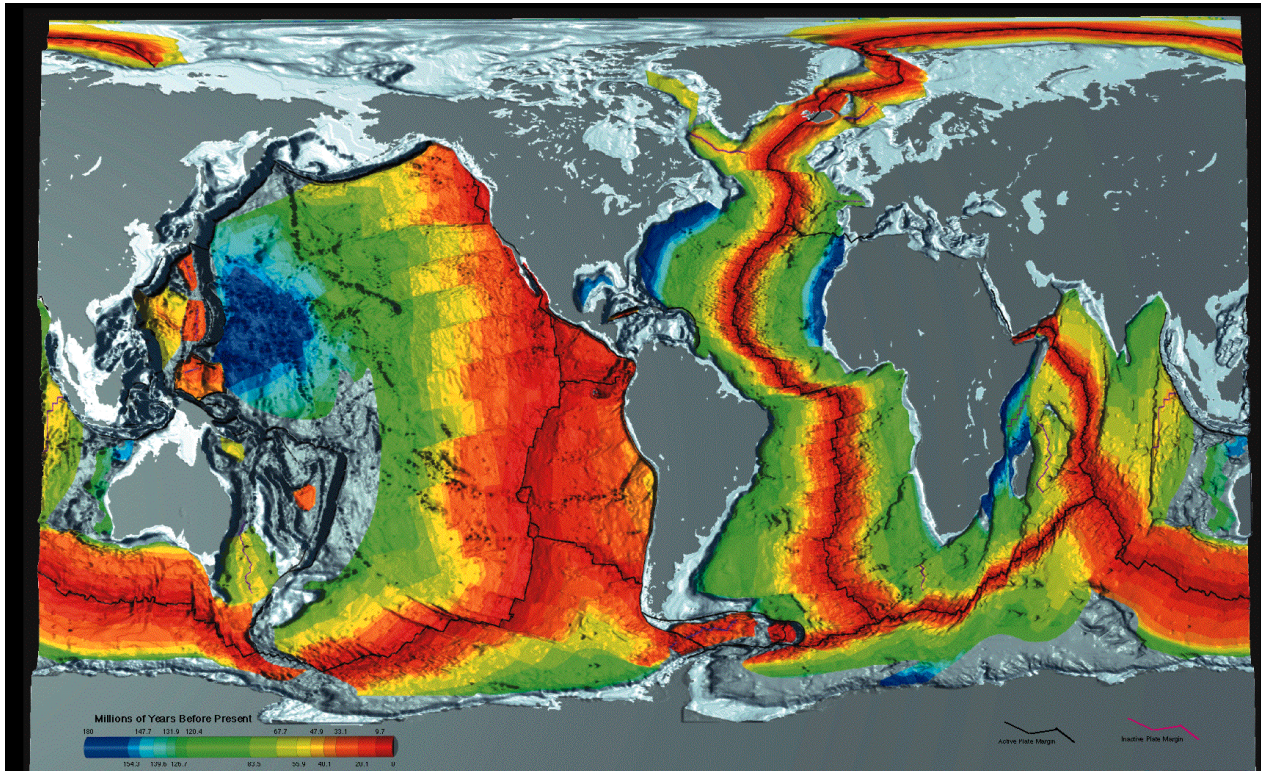


Fast=Twice the present spreading rates and oldest sea floor 90 Myr.
Uniform=uniform distribution of ages from 0 to 90 Myr with the same spreading rate as present.

- Oceanic heat loss depends on the distribution of sea-floor ages (rate of sea-floor creation/destruction)
- Additional contribution of hot spots (areas of enhanced heat flux) to the heat loss are not included (2-4 TW)

Oceanic heat loss

- Changes of oceanic heat loss can occur when a new ridge forms (it enhances heat loss, due to an increase of area of young sea floor), when a new subduction zone appears (it reduces heat loss) and, more in general, when the spreading rates change.
- The Pacific ocean alone accounts for almost 50% of the oceanic total and 34% of the global heat loss of the planet, due to its high spreading rate. The Atlantic ocean started to open 180 Myr and its heat loss is ~ 6 TW, 17% of the oceanic total.
- Using the half-space cooling model, the distribution of the sea-floor age f is a function of the ratio τ/τ_m .



$$\frac{dA}{d\tau} = C_A f \left(\frac{\tau}{\tau_m} \right) \quad Q_{oc} = A_o \frac{\lambda T_M}{\sqrt{\pi \kappa \tau_m}} \gamma(f)$$

A_o =total ocean surface, C_A =plate accretion rate, $f(0)=1$
 τ =time, τ_m =maximum age, $\gamma(f)$ =coefficient depending on the dimensionless age distribution (τ/τ_m).

$$Q_{oc}^T = \frac{8A_o}{3} \frac{\lambda T_M}{\sqrt{\pi \kappa \tau_m}} \quad Q_{oc}^R = 2A_o \frac{\lambda T_M}{\sqrt{\pi \kappa \tau_m}}$$

Triangular age distribution

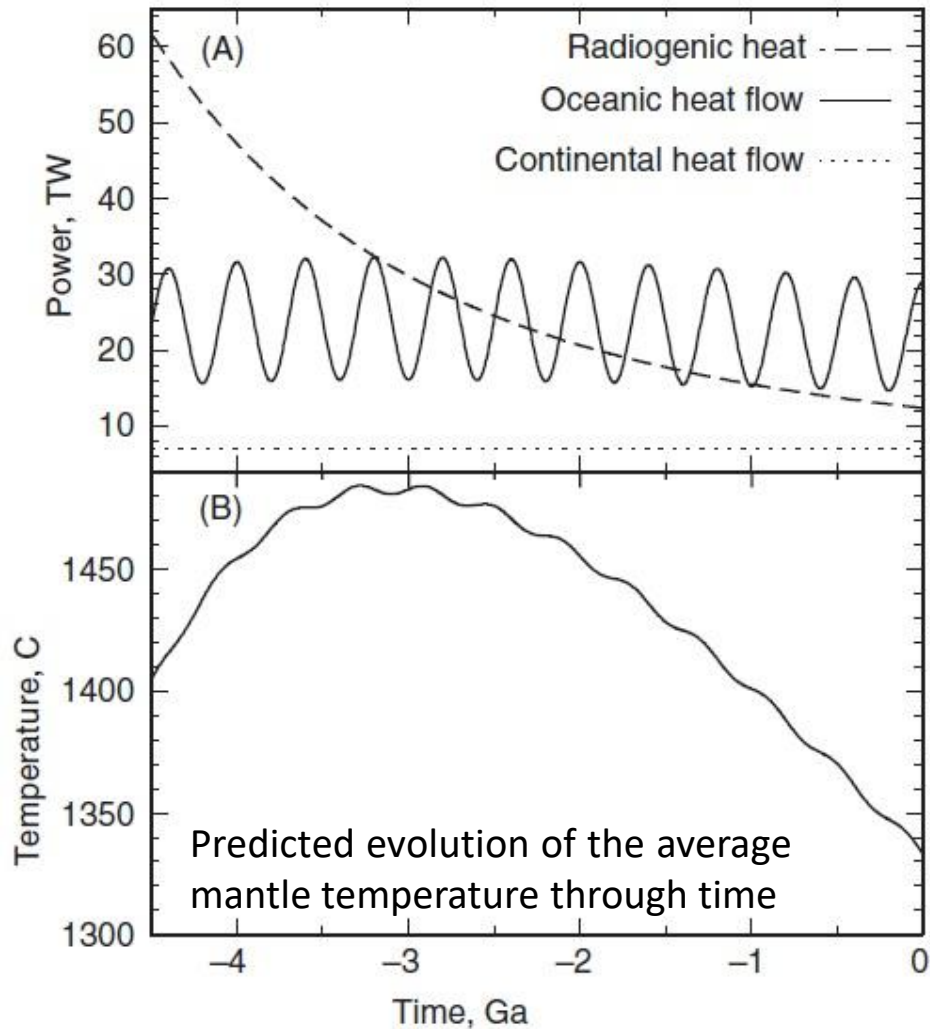
Rectangular age distribution

Heat loss increases by 30%

- Changing that sea-floor age distribution can change the oceanic heat loss. The sea-floor spreading seems to proceed with a rectangular age distribution in ocean basins that do not exceed a certain size (younger than 110 Myr): In the Atlantic Ocean the age distribution is rectangular up to 80 Myr, and then the area per unit age decreases for older age, while the Pacific ocean shows no simple age distribution.

Oceanic heat loss

The evolution of the oceanic plates leads to significant short-term variations of heat loss and mantle temperatures



$$Q_{oc} = A_o \frac{\lambda T_M}{\sqrt{\pi \kappa \tau_m}} \gamma(f)$$

τ_c = time scale for the cooling of the Earth through the oceans

$$\tau_c = \frac{MC_p T_M}{Q_{oc}} = \frac{MC_p \sqrt{\pi \kappa \tau_m}}{\lambda A_o \gamma(f)}$$

τ_c = time required for both temperature and heat flux to drop by a factor e if all heat sources are instantly suppressed ($\tau_c \sim 10$ Gyr).

- Fluctuations of heat loss must be spread over time intervals that are not short compared to τ_c to affect the average mantle T .
- Fluctuation of heat loss due to plate reorganizations of time scale $\tau_w \sim 400$ Myr does not affect significantly the secular cooling trend, neither the mantle temperatures.

Mantle Heat Production

- From the different models for the bulk silicate Earth, the total rate of heat production is ~20 TW. After removing the contributions of the continental crust (6–7 TW) and the lithospheric mantle (~1 TW), heat production in the mantle amounts to a total of 13 TW.

Radioelement concentration and heat production in meteorites, in the bulk silicate Earth, the Earth's mantle and crust

	U (ppm)	Th (ppm)	K (ppm)	A* (pW kg ⁻¹)
CI chondrites				
Palme and O'Neill (2003)	0.0080	0.030	544	3.5
McDonough and Sun (1995)	0.0070	0.029	550	3.4
Bulk silicate Earth				
From CI chondrites				
Javoy (1999)	0.020	0.069	270	4.6
From EH chondrites				
Javoy (1999)	0.014	0.042	385	3.7
From chondrites and lherzolites trends				
Hart and Zindler (1986)	0.021	0.079	264	4.9
From elemental ratios and refractory lithophile elements abundances				
McDonough and Sun (1995)	0.020 ± 20%	0.079 ± 15%	240 ± 20%	4.8 ± 0.8
Palme and O'Neill (2003)	0.022 ± 15%	0.083 ± 15%	261 ± 15%	5.1 ± 0.8
Lyubetskaya and Korenaga (2006)	0.017 ± 0.003	0.063 ± 0.011	190 ± 40	3.9 ± 0.7
Depleted MORB source				
Workman and Hart (2005)	0.0032	0.0079	25	0.59
Average MORB mantle source				
Su (2000); Langmuir <i>et al.</i> (2005)	0.013	0.040	160	2.8
Continental crust				
Rudnick and Gao (2003)	1.3	5.6	1.5 × 10 ⁴	330
Jaupart and Mareschal (2003)	/	/	/	293–352

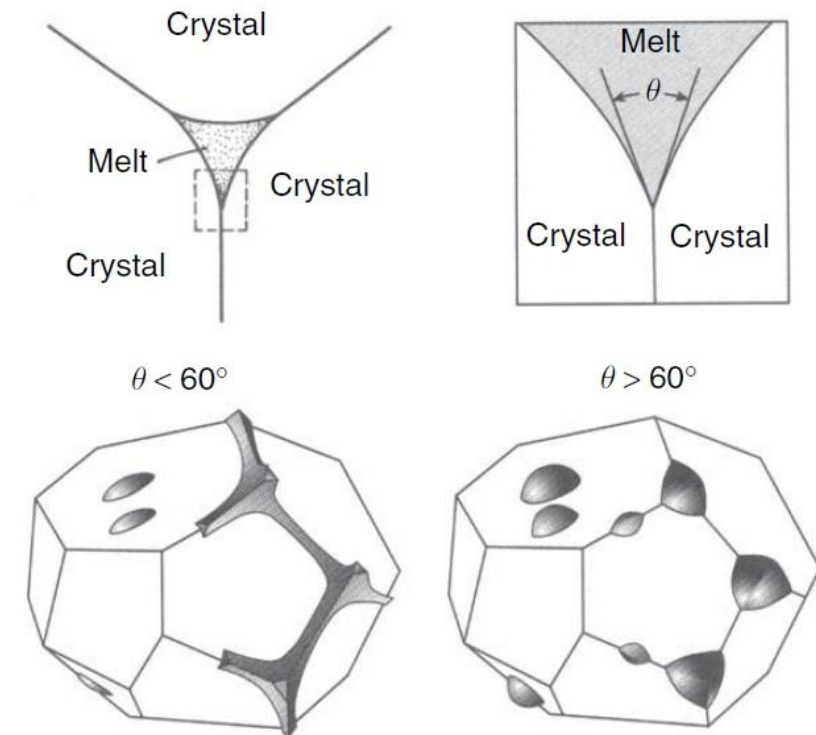
Earth's core formation

- When more than 60% of the magma oceans crystallized the iron was transported towards the center of the planet. The transport mechanism might be percolation through a partially molten mantle, or the motion of larger iron bodies via brittle fractures (dyking) or through a viscously deformable mantle (diapirism).
- The redistribution of mass involved with the descent of iron toward the center of the planet results in a release of gravitational energy. The process involved the transport of liquid metal through either solid (crystalline) silicates (possible, since has a lower melting temperature than mantle silicates) or through partially or fully molten silicate (i.e., in a magma ocean).

Ways of iron transportation: Percolation

Liquid metal can percolate through a matrix of polycrystalline silicates by porous flow provided the liquid is interconnected ($\theta < 60^\circ$) and does not form isolated pockets ($\theta > 60^\circ$).

- The dihedral angle (θ), can be affected by (1) the structure and composition of the crystalline phase, (2) the structure and composition of the liquid metal alloy, and (3) temperature and pressure.
- Experimental results for systems under hydrostatic stress show that θ angles significantly exceed the critical angle of 60° at P of 3–25GPa and thus percolation is not applicable to the core formation.

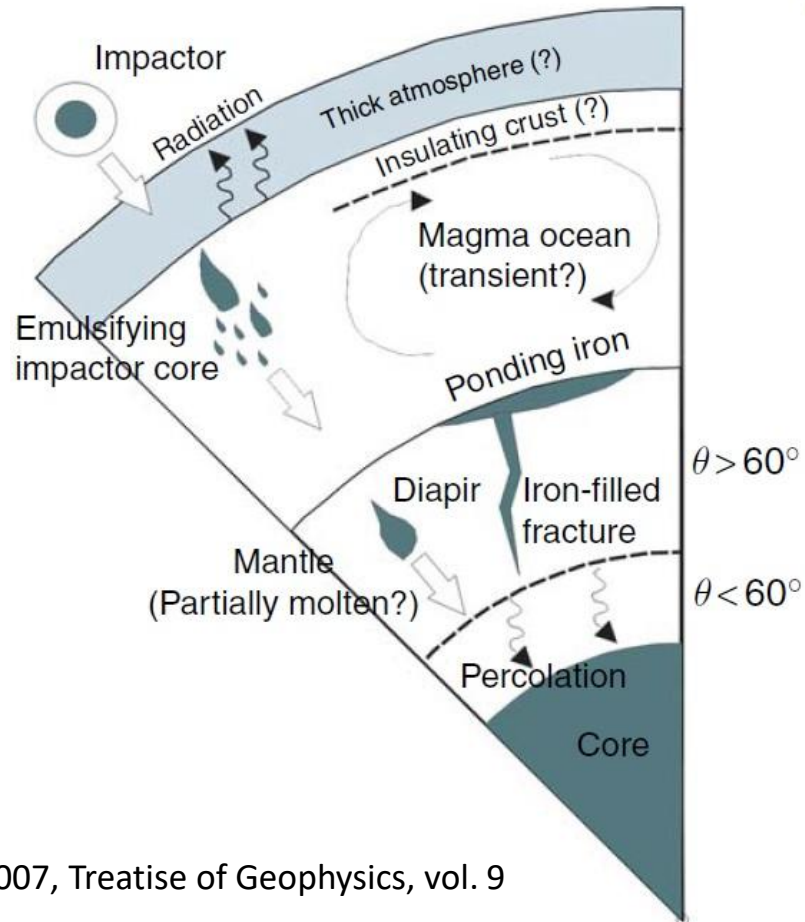


Earth's core formation

Ways of iron transportation: Diapirs

- When liquid iron ponds as a layer at the base of a magma ocean, gravitational instabilities develop due to the density contrast with the underlying silicate-rich material and cause diapir formation.
- Their size and rate of descent through the mantle depend on the initial thickness of the metal layer and the viscosity of the silicate mantle. Gravitational heating will be important and will facilitate diapir descent by reducing the viscosity of the adjacent mantle.

Ways of iron transportation: Dyking

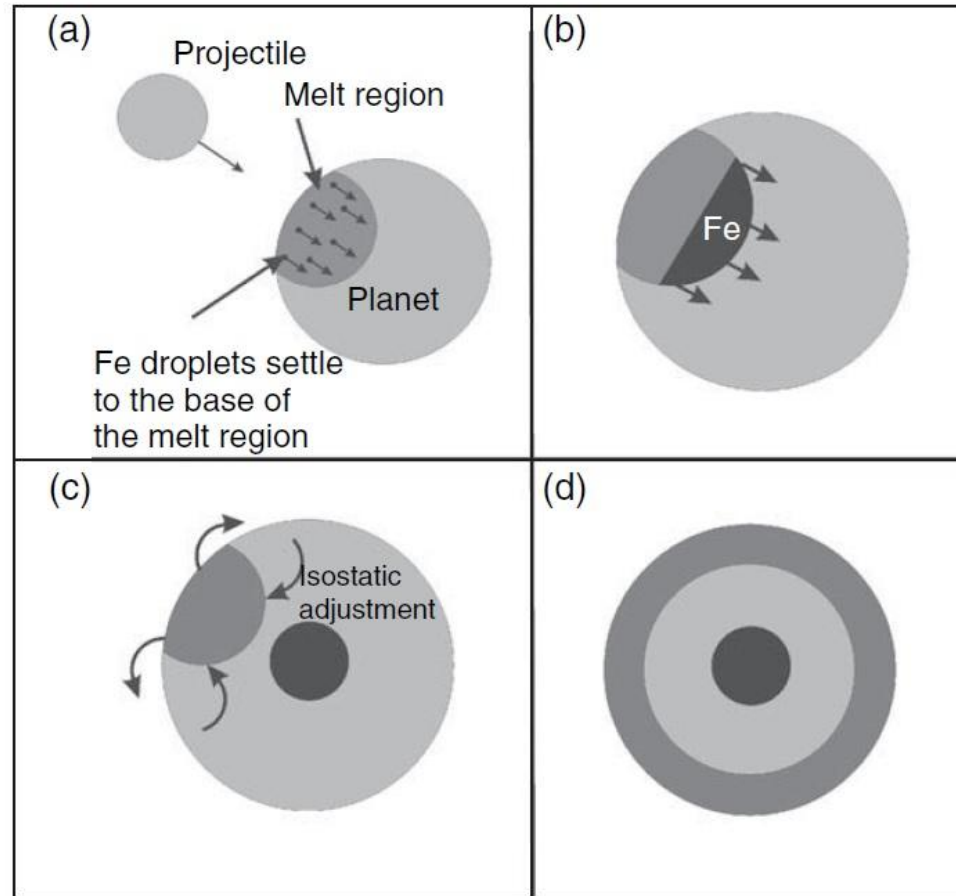


- Dykes can form and propagate in the hot mantle underlying the magma ocean, so long as the contrast in viscosity between the fluid in the dyke and the surrounding host rocks is greater than 10^{11} – 10^{14} Pa s.
- With a viscosity in the liquid iron of 10^{-2} Pa s, is thus expected to form dykes if the viscosity of the host rock exceeds 10^9 – 10^{12} Pa s.
- Liquid metal separates rapidly from liquid silicate in a deep magma ocean and accumulates as ponded layers at the rheological base of the magma ocean.
- The ponded iron then migrates through the largely crystalline underlying mantle towards the proto-core by either percolation, diapirism, or dyking.

Earth's core formation

Alternative Hypothesis:

- (a)** Initially a magma ocean, generated by a large impacts, is initially a hemispherical body of limited lateral extent.
 - (b-c)** There is the possibility that iron, emulsified in the form of small dispersed droplets (~1cm), settles and segregates rapidly to form a protocore at the bottom of this magma ocean.
 - (d)** Subsequent isostatic adjustment causes the magma ocean to evolve into a layer of global extent.
- The gravitational energy of sinking droplets is converted into heat which raises the temperature at the base of the magma ocean by at least several hundred degrees.



Core Composition

- The density of the Earth's core is too low, by 5–10%, for it to consist only of *Fe* and *Ni* and thus the core must contain up to 10 wt.% of one or more light elements (e.g., *S*, *O*, *Si*, *C*, *P*, and *H*).
- The expulsion of light elements in the outer core generates compositional convection which helps to drive the geodynamo and decreases the melting temperature of the core by several hundred degree. Identification of the light elements can constrain the conditions under which the core is formed.
- Oxygen, due to its small atomic radius, tends to be expelled during the freezing of liquid iron. Conversely, *S* and *Si* have atomic radii similar to that of iron at core pressures, and thus substitute freely for iron in the solid inner core.
- Because oxygen solubility in liquid *Fe* increases strongly with temperature, FeO partitions increasingly into the *Fe* alloy as the magma ocean depth is increased beyond 1000 km, leaving the silicate depleted in FeO. This hypothesis is consistent with equilibration in a magma ocean 1200–2000 km deep and with the Earth's core containing 7–8 wt.% oxygen.
- There are isotopes (¹⁸⁷Re and ¹⁹⁰Pt) that partition preferentially into the outer core and decay to ¹⁸⁷Os and ¹⁸⁶Os. The outer core becomes enriched in these Os isotopes relative to stable ¹⁸⁸Os. The elevated Os-isotope ratios in the komatiites would be indicative of early core solidification (3.5 Gyr).

Table Model core compositions

	MA	WD	A+	McD-1	McD-2
Fe (wt.%)	84.5	80.3	79.4	85.5	88.3
Ni	5.6	5.5	4.9	5.2	5.4
Si	–	14.0	7.4	6.0	–
S	9.0	–	2.3	1.9	1.9
O	–	–	4.1	–	3.0
C	–	–	–	0.2	0.2
Co	0.26	0.27	0.25	–	–

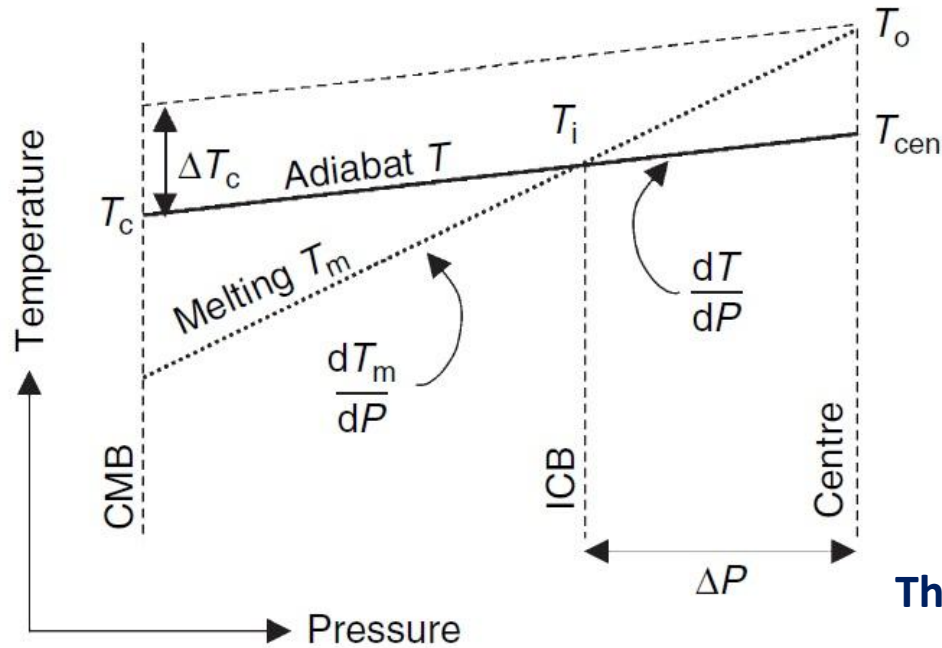
MA=Morgan and Anders 1980; WD=Wanke and Dreibus 1988; A+=Allegre et al. 1995a; McD-1 and McD-2 refer to two different models given in McDonough (2003).

Nimmo, 2007, Treatise of Geophysics, vol. 9

MA = Morgan and Anders 1980; WD = Wanke and Dreibus 1988; A+ = Allegre *et al.* 1995a; McD-1 and McD-2 refer to two different models given in McDonough (2003).

These models are derived by comparing estimates of the bulk silicate Earth elemental abundances, with estimates of the initial solar nebular composition (based mainly on chondritic meteorite samples).

Core temperature



Nimmo, 2007, Treatise of Geophysics, vol. 9

	Model					Eq.	Model				
	1	2	3	Units			1	2	3	Units	Eq.
k	20	40	60	$\text{W m}^{-1} \text{K}^{-1}$	2.2	$\Delta\rho_c$	600	400	200	kg m^{-3}	2.1
ΔT_c	150	100	50	K	(7)	α	0.8	1.35	1.9	$\times 10^{-5} \text{K}^{-1}$	(5)
D	7754	5969	5031	km	(5)	T_{cen}	4893	5619	6454	K	(4)
T_i	4773	5389	6085	K	2.4	T_o	5076	5760	6535	K	2.4
T_{m0}	1460	1322	1165	K	(6)	dT_m/dP	10.1	12.4	15.0	K GPa^{-1}	(6)
Q_k	1.4	4.8	10.0	TW	(12)	\tilde{Q}_T	2.9	3.2	3.8	$\times 10^{27} \text{J}$	(11)

Models 1 and 3 are end-member cases using parameter values designed to generate ancient and recent inner cores. Model 2 is a best guess at the real parameter values.

T_{m0} incorporates the reduction in melting temperature due to the light element

The adiabatic temperature T within the core is given by: $T(r) = T_{\text{cen}} \exp(-r^2/D^2)$

$T_i = 5650 \pm 600 \text{ K}$ $r = \text{distance to the centre of the Earth}$

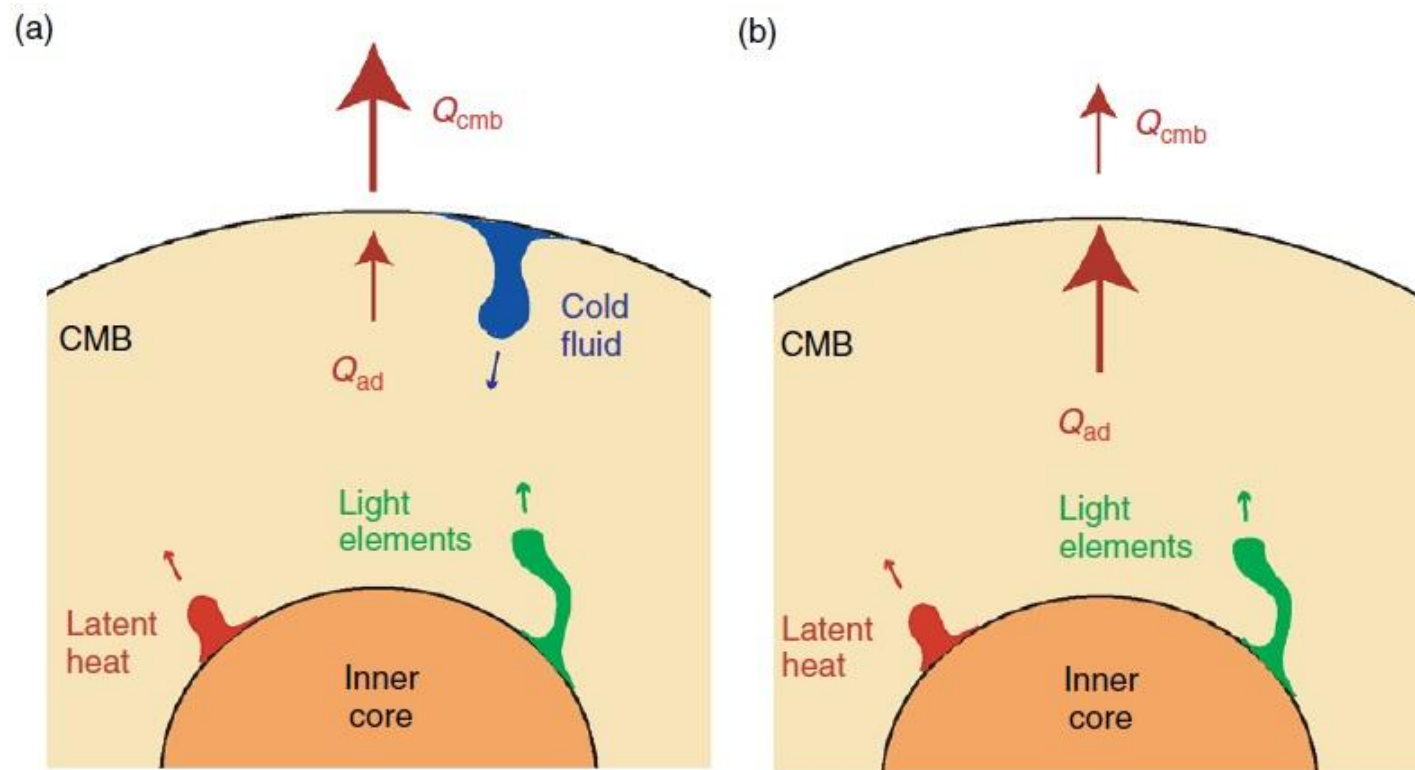
$G = \text{universal gravitational constant}$

$$D = \sqrt{3C_p/2\pi\alpha\rho_{\text{cen}}G}$$

- As long as the core is convecting, its mean T profile will be that of an adiabat, except at the very thin top and bottom boundary layers (D'' layer). Since the T at the ICB must equal the melting T of the core at that pressure, the T elsewhere in the core may be extrapolated from the ICB conditions by using the appropriate adiabat.
- T at the bottom of D'' layer (the core) arises from extrapolating the T at the ICB outwards along an adiabat, and is about 4000K. T at the top of the D'' layer is obtained from extrapolating the mantle potential T inwards along an adiabat, and is about 2700K.
- The CMB region may include a phase transition to a postperovskite structure which will also affect the CMB heat flux.
- The earliest documented apparent paleomagnetic reversal is dated at 3.2 Gyr and can be used to constrain the evolution of the core over time.
- Theoretical estimates suggest that the inner core probably formed at 1 Gyr, but according to the Re–Os–Pt isotopic system the inner-core solidification started by 3.5 Gy BP.
- The CMB heat flux has likely evolved in two stages: an early, high heat flux stage, presumably due to the melting of the lower mantle, and potentially generating very strong magnetic fields and a later, lower heat flux stage.

Core-Mantle Interaction

- Heat flow across the core–mantle boundary (CMB) controls the rate of cooling and solidification of the core, and determines the vigor of convection in the fluid outer core.
- Chemical buoyancy of the outer core arises through the exclusion of the light elements from the inner core, while thermal buoyancy is generated by latent heat release on solidification and by forming cold, dense fluid in the thermal boundary layer at the top of the core.
- **Two different styles of convection in the core can occur:** **(1)** when the Q_{cmb} exceeds the conduction of heat along the adiabatic gradient at the top of the core (Q_{ad}). Convection transports the superadiabatic part of heat flow through the core, creating a thermal boundary layer on the core side of the boundary. This provides a source of cold, dense fluid that drives convection from the top down into the core; **(2)** when the Q_{cmb} is less than Q_{ad} . In this case, the mantle is unable to remove the heat carried by conduction down the adiabat. Excess heat accumulates at the top of the core or is convectively mixed into the interior by chemical buoyancy



Heat flow out of the core

- The core loses heat to an unstable boundary layer which grows at the base of the mantle (D'' layer).
- The T difference across this 200 km thick layer is about $\delta T = 1000\text{K}$.
- The energy balance of the core equates the heat flux at the CMB to the sum of secular cooling, Q_s , latent heat from inner-core crystallization, Q_L , gravitational energy due to chemical separation of the inner core, Q_g , and radiogenic heat generation, Q_R .
- Secular cooling makes the inner core grow, which releases latent heat and compositional energy, which are related to the size of the inner core and its growth rate (300 kmGyr^{-1}).

$$Q_{\text{cmb}} = Q_s + Q_g + Q_L + Q_R$$

The energy content of the D'' layer, transferred to the mantle when the boundary layer goes unstable, is:

$$U = \rho C_p 4\pi b^2 h \frac{\delta T}{2} \simeq 7.5 \cdot 10^{28} \text{ J}$$

$$b = \text{radius of the core } 3480 \text{ km}, \rho = \sim 5 \times 10^3 \text{ kgm}^{-3} \quad h = 200 \text{ km} \quad C_p = 1000 \text{ Jkg}^{-1}\text{K}^{-1} \quad \delta T = 1000 \text{ K}$$

Time scale of the energy release to the mantle is that of conductive thickening of the layer: $\tau = h^2 / \pi \kappa \sim 400 \text{ Myr}$, for $\kappa = 10^{-6} \text{ m}^2 \text{ s}^{-1}$

- Dividing the total energy in the thermal boundary layer by the time scale of 400 Myr indicates that the variations of heat input at the base of the mantle is $\sim 5 \text{ TW}$.
- **Total heat flux across the CMB = 7-14 TW** (sum of secular cooling, latent heat from inner core crystallization, compositional energy due to chemical separation of the inner core, radiogenic heat generation).
- An independent estimate of $13 \pm 4 \text{ TW}$ was derived from the post-perovskite phase change and an estimate of thermal conductivity at the base of the mantle.

Mantle Thermal evolution

- Over the Earth history, heat sources have decreased by a factor of ~ 4 . The decay time of bulk radiogenic heat production (the weighted average of the individual decay times of the main isotopes) is 3Gyr.
- The efficiency of the Earth's convective engine in losing the heat is given by the Urey (Ur) ratio (ratio of the rate of heat production over the rate of heat loss).

$$Ur = 0.33-0.43 \quad Ur = \frac{\int_V H dV}{\int_A \mathbf{q} \cdot \mathbf{n} dA} = \frac{H_T}{Q}$$

Q =total rate of heat loss

H_T =Total heat production rate

For $Ur=1$, mantle T remains constant

From the present-day energy budget, the cooling rate is $\sim 120 \text{ K Gyr}^{-1}$ ($> 50 \text{ K Gyr}^{-1}$): cooling rate is increased with time

The global heat balance is:

$$M \langle C_p \rangle \frac{d\langle T \rangle}{dt} = -Q + H_T \quad \frac{Q_{av} - H_{Tav}}{Q - H_T} = \frac{(dT/dt)_{av}}{d\langle T \rangle/dt} \quad \text{Ur} \sim 0.4 \text{ (rate of } Q \text{ varies less rapidly than that of } H_T)$$

By integrating over the age of the Earth

Q_{av} = time-averaged of heat loss

H_{Tav} = time-averaged of heat production

$\langle C_p \rangle$ = "effective" heat capacity which accounts for the variation of temperature with depth

$(dT/dt)_{av}$ = average cooling rate

Heat loss of the Earth

How the continental growth does influence the cooling of the Earth?

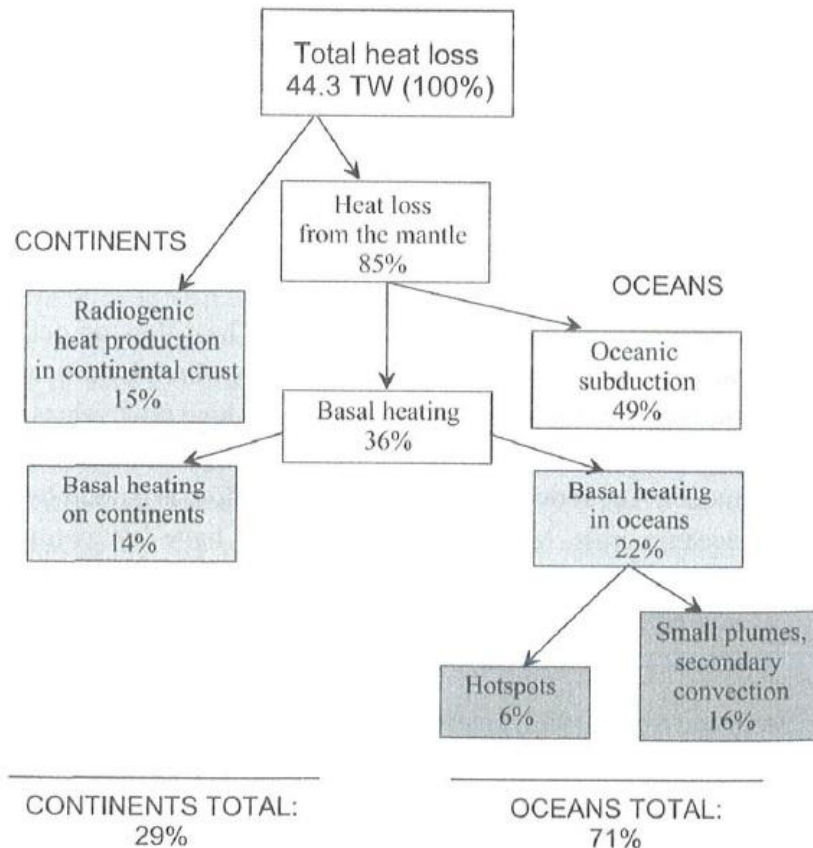
Continental growth reduces the Earth's cooling rate, since (1) it acts to reduce the amount of internal heat generation driving mantle convection (by the extraction of radioelements from the mantle), (2) it increases the size of continental domain at the expenses of the oceanic one, (3) convection cells stretch over larger horizontal distance implying a lower heat flux than with the shorter cells.

Total heat loss from ocean = 32TW

Total heat loss from continents = 14 TW

Total heat loss from continental crust = 6-7 TW (resulting from a crustal range of heat production $0.79\text{-}0.99 \mu\text{Wm}^{-3}$ and volume $0.73 \times 10^{10} \text{ km}^3$)

Total heat loss from cont. lithospheric mantle = 0.5 TW (resulting from a mantle range of heat production 0.02 mWm^{-3} and volume $3.1 \times 10^{10} \text{ km}^3$)



Heat flow balance of the Earth			
Source of heat	Mean surface heat flow* (mW/m ²)	Heat loss (TW)**	Total global heat loss (%)
Continents (area $2.0 \times 10^8 \text{ km}^2$)	65.0 ± 1.6	13.0 ± 0.3	29.3
<i>Radiogenic heat production in continental crust</i>	34 ± 8	6.8 ± 1.6	15.3
<i>Basal heating of continental lithosphere</i>	31 ± 8	6.2 ± 1.6	14.0
Oceans and marginal basins (area $3.1 \times 10^8 \text{ km}^2$)	101.0 ± 2.2	31.3 ± 0.7	70.7
<i>Subduction of oceanic lithosphere</i>	70 ± 8	21.7 ± 2.5	49.0
<i>Basal heating of oceanic lithosphere</i>	31 ± 8	9.6 ± 2.5	21.7
Total global	86.9 ± 2.0	44.3 ± 1.0	100

(after Malamud and Turcotte, 1999)
 * Sources: Sclater *et al.*, 1980; Pollack *et al.*, 1993
 ** 1TW=10¹² W

- ~65% of present global heat is lost by convection (which includes oceanic plate creation and continental orogenies), ~20% by conduction, and the remaining ~15% by radioactive decay of heat-producing elements in the crust.

References

Main Readings:

Books:

- Artemieva, 2011, Chapter 4, Thermal regime of the lithosphere from heat flow data, The lithosphere an interdisciplinary approach, Cambridge and University Press.
- Jaupart and Mareshal, 2011, Heat Generation and Transport in the Earth , Chapter 8: Global Energy Budget, Crust, mantle, and core,
- Jaupart and Mareshal, 2011, Heat Generation and Transport in the Earth , Chapter 10: Thermal evolution of the Earth
- Jaupart and Labrosse, 2007, Treatise of Geophysics, vol. 7, Temperatures, Heat and Energy in the Mantle of the Earth, 253-303.
- Nimmo, 2007, Treatise of Geophysics, vol. 9, Thermal and Compositional Evolution of the Core, 217-241

Further Readings:

- Buffett, 2007, Core–Mantle Interactions, Teatise of Geopysics, vol. 8.
- Rubie et al., 2007, Treatise of Geophysics, Formation of Earth's Core, vol. 9, 51-90.